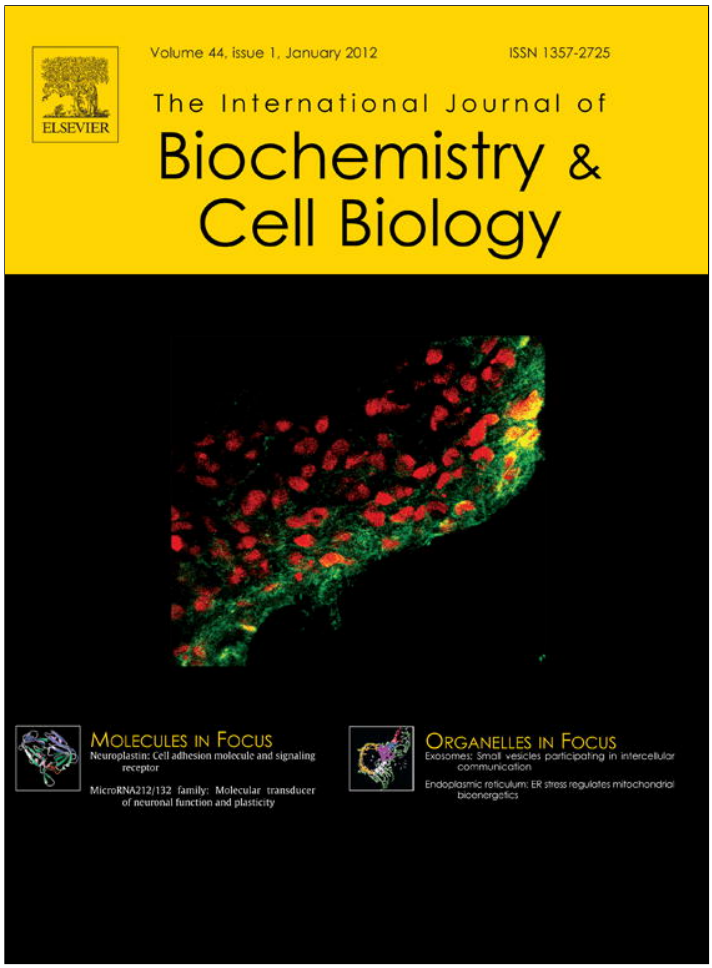

The International Journal of Biochemistry & Cell Biology 45 (2013) 1927–1938

Contents lists available at SciVerse ScienceDirect

The International Journal of Biochemistry & Cell Biology

journal homepage: www.elsevier.com/locate/biocel

Dysferlin interacts with calsequestrin-1, myomesin-2 and dynein in human skeletal muscle

Bàrbara Flix[a,b], Carolina de la Torre[c], Juan Castillo[a,b], Carme Casal[d], Isabel Illa[a,b], Eduard Gallardo[a,b,*]

[a] Servei de Neurologia, Laboratori de Neurologia Experimental, Hospital de la Santa Creu i Sant Pau i Institut de Recerca de HSCSP, C/ S.A.M. Claret 167, 08025 Barcelona, Spain
[b] Universitat Autònoma de Barcelona and Centro de Investigación Biomédica en Red de Enfermedades Neurodegenerativas (CIBERNED), Spain
[c] Plataforma de serveis científico-tècnics de l'Hospital de Vall d'Hebron, Servei de proteòmica, Passeig de la Vall d'Hebron, 119, 08035 Barcelona, Spain
[d] Plataforma de serveis científico-tècnics del HSCSP, Servei de microscopia, C/ S.A.M. Claret 167, 08025 Barcelona, Spain

ARTICLE INFO

Article history:
Received 5 March 2013
Received in revised form 24 May 2013
Accepted 9 June 2013
Available online xxx

Keywords:
Dysferlin
FLIM–FRET analysis
Blue native
Cytoplasmic dynein
Trim72/MG53

ABSTRACT

Dysferlinopathies are a group of progressive muscular dystrophies characterized by mutations in the gene DYSF. These mutations cause scarcity or complete absence of dysferlin, a protein that is expressed in skeletal muscle and plays a role in membrane repair. Our objective was to unravel the proteins that constitute the dysferlin complex and their interaction within the complex using immunoprecipitation assays (IP), blue native gel electrophoresis (BN) in healthy adult skeletal muscle and healthy cultured myotubes, and fluorescence lifetime imaging–fluorescence resonance energy transfer (FLIM–FRET) analysis in healthy myotubes. The combination of immunoprecipitations and blue native electrophoresis allowed us to identify previously reported partners of dysferlin – such as caveolin-3, AHNAK, annexins, or Trim72/MG53 – and new interacting partners. Fluorescence lifetime imaging showed a direct interaction of dysferlin with Trim72/MG53, AHNAK, cytoplasmic dynein, myomesin-2 and calsequestrin-1, but not with caveolin-3 or dystrophin. In conclusion, although IP and BN are useful tools to identify the proteins in a complex, techniques such as fluorescence lifetime imaging analysis are needed to determine the direct and indirect interactions of these proteins within the complex. This knowledge may help us to better understand the roles of dysferlin in muscle tissue and identify new genes involved in muscular dystrophies in which the responsible gene is unknown.

1. Introduction

Dysferlinopathies, also called dysferlin myopathies, are a heterogenous group of progressive muscular dystrophies characterized by mutations in the DYSF gene (Bashir et al., 1998; Liu et al., 1998). These mutations produce reduced or null expression of the dysferlin protein and can cause a variety of phenotypes (Illa et al., 2007, 2001; Nguyen et al., 2007; Paradas et al., 2009; Passos-Bueno et al., 1995), such as limb girdle muscular dystrophy type 2B (LGMD2B) (Bashir et al., 1996) or Miyoshi myopathy (MM) (Miyoshi et al., 1986). Dysferlin myopathies present with muscle weakness and high levels of creatinin kinase in serum, and the muscle biopsy shows dystrophic features and inflammatory infiltrates. There is no correlation, however, between the kind of mutation and a particular phenotype (Krahn et al., 2009). Moreover, all phenotypes show a similar MRI pattern (Paradas et al., 2010).

Dysferlin is a type II protein with a short extracellular tail. It is expressed in several tissues such as monocytes, heart, placenta, liver, lungs, pancreas and kidney (Liu et al., 1998), but most studies focus on skeletal muscle where it plays an essential role in sarcolemma repair (Bansal and Campbell, 2004). In skeletal muscle, dysferlin is expressed in the sarcolemma, in intracellular vesicles and in t-tubules (Glover and Brown, 2007). The analysis of proteins interacting with dysferlin has been addressed in several studies. Most such studies are based on co-immunoprecipitation assays (IP). Co-IP assays have led to the discovery of several dysferlin partners, such as AHNAK (Huang et al., 2007), Trim72/MG53 (Cai et al., 2009b), caveolin-3 (Cav-3) (Matsuda et al., 2001), and

Abbreviations: CALQ1, calsequestrin-1; Cav-3, caveolin-3; DHPR, dihydropyridine receptor; DMD, Duchenne muscular dystrophy; DYNC1LI2, cytoplasmic dynein 1 light intermediate chain 2; FLIM–FRET, fluorescence lifetime imaging–fluorescence resonance energy transfer; FSHD, fascio-scapulo-humeral dystrophy; HAC6, histone deacetylase 6; LGMD1C, limb girdle muscular dystrophy 1C; LGMD2B, limb girdle muscular dystrophy 2B; MM, Miyoshi myopathy; MYOM2, myomesin-2; PTRF, polymerase I and transcript release factor; RRC, receptor recycling compartment; SERCA, sarcoplasmic/endoplasmic reticulum calcium ATPase; SR, sarcoplasmic reticulum; trim72/MG53, tripartite containing motif 72/mitsugumin 53.

* Corresponding author at: Department of Neurology, Hospital de Sant Pau, C/ S.A.M. Claret 167, 08025, Barcelona, Spain. Tel.: +34 93 5567692; fax: +34 93 2919275.
E-mail address: egallardo@santpau.cat (E. Gallardo).

1357-2725/$ – see front matter © 2013 Elsevier Ltd. All rights reserved.
http://dx.doi.org/10.1016/j.biocel.2013.06.007

Vinculin (de Morree et al., 2010). These techniques are used to determine which proteins belong to a certain complex but they do not add information on direct or indirect interactions, as two proteins that co-IP do not necessarily interact directly. One of the proteins reported to belong to the dysferlin is AHNAK. It is an enlargeosome marker that colocalizes with dysferlin at the plasma membrane. In the absence of dysferlin, levels of AHNAK are decreased in the sarcolemma (Zacharias et al., 2011). AHNAK participates in membrane repair, vesicle trafficking, and excitation-contraction coupling in skeletal muscle and other tissues (Borgonovo et al., 2002; Haase et al., 1999; Hohaus et al., 2002). The interaction is calcium-independent and mediated by calpain 3 proteolysis (Huang et al., 2008).

Another known partner for dysferlin is Trim72/MG53, a protein that plays a key role in rapid repair of wounded membrane in a Ca^{2+} independent manner (Cai et al., 2009a). It has been reported that Trim72/Mg53 trafficking to the membrane injury site requires polymerase I and transcript release factor (PTRF) (Zhu et al., 2011). PTRF is a protein related to caveolae that is also present in the dysferlin complex (Cacciottolo et al., 2010). Cav-3 is also present in caveolae (Matsuda et al., 2001) and its absence causes limb girdle muscular dystrophy type 1C (LGMD1C) (Minetti et al., 1998). This dominant muscular dystrophy presents reduced levels of Cav-3 in the muscle biopsy, and in some cases, it also shows a secondary reduction of dysferlin (Matsuda et al., 2001), possibly because mutations in CAV3 gene increase dysferlin endocytosis (Hernandez-Deviez et al., 2008). It has been shown that Cav-3 co-immunoprecipitates not only with dysferlin but also with Trim72/MG53 and that this complex has an important role in membrane repair (Cai et al., 2009b). Dysferlin and Cav-3 are also present in the t-tubules, where they colocalize with the dihydropyridine receptor (DHPR) (Ampong et al., 2005). In addition, dysferlin and cav-3 participate in myoblast fusion to form myotubes (Madaro et al., 2011; De Luna et al., 2004; de Luna et al., 2006), a process that requires integrins. Along the same lines, it has been shown that dysferlin interacts with affixin (beta-parvin) and vinculin. These two proteins link dysferlin to integrins and support the role of dysferlin in sarcolemma integrity (Matsuda et al., 2005; de Morree et al., 2010).

In a very recent work, it was shown that dysferlin interacts with tubulin (Azakir et al., 2010) and histone deacetylase 6 (HAC6) (Di Fulvio et al., 2011). The authors related this interaction to muscle differentiation as they observed that dysferlin promoted alpha-tubulin acetylation, preventing HDAC6 activity by binding both proteins. It has previously been reported that a high acetylation state of alpha-tubulin is needed for the microtubule elongation and stabilization required for myogenesis and myotube elongation (Di Fulvio et al., 2011).

Fluorescence lifetime imaging–fluorescence resonance energy transfer (FLIM–FRET) analysis is the most robust way to demonstrate direct interactions between two proteins (Sun et al., 2011; Badiola et al., 2011; Guardia-Laguarta et al., 2009; Lennon et al., 2003). Using this technique, Lennon et al. (2003) showed that dysferlin interacts directly with annexin A1 and with annexin A2, the only direct interactions for dysferlin described to date. The authors showed that these interactions require the presence of calcium, and also that the interaction of annexin A1 and dysferlin is disrupted after sarcolemmal injury. To further understand the different functions of dysferlin it is necessary to determine if there are other proteins present in the dysferlin complex. Moreover, dysferlin partners are putative genes causing non-filiated dystrophies and could help to understand the phenotypic variability in dysferlinopathies.

The aims of our study were, first, to find new members of the dysferlin interactome by combining three techniques: IP, blue native electrophoresis (BN), and FRET–FLIM analysis; and second, to distinguish whether proteins in the dysferlin complex interact directly or indirectly.

2. Materials and methods

2.1. Primary muscle cultures

Human muscle biopsies were minced and cultured in monolayer following the method described by Dr. Askanas (Askanas et al., 1971) with some modifications (De Luna et al., 2004). The culture media for myoblast proliferation contains 75% DMEM and 25% M199, complemented with 10% Fetal bovine serum (FBS), 10 μg/ml insulin, 2 mM glutamine and penicillin–streptomycin–fungizone, 10 ng/ml epidermal growth factor and 25 ng/ml fibroblast growth factor. Cells were grown to 80% confluence. The culture media was then substituted for one without growth factors and with only 2% of FBS.

To injure cells, myotubes were treated with 0.25 mM SDS for 2 min at 37 °C and fixed with cold methanol for 10 min.

2.2. Biopsies

Blue native experiments were performed using a muscle biopsy from the semitendinous muscle of a healthy patient. The immunoprecipitation assays were performed using muscle biopsies from a vastus externus and a facia lata from healthy patients. All patients signed an informed consent and the project was approved by the Ethics Committee at Hospital de la Santa Creu i Sant Pau (code 12/2009).

2.3. Immunoprecipitation assays

Protein extracts from myotubes and adult skeletal muscle were obtained by sonication in a lysis buffer containing 50 mM Tris–HCl, pH 7.5, 150 mM NaCl, 0.2% Triton X-100 and 1× protease inhibitor cocktail (GE Healthcare Lifesciences, Freiburg, Germany) on ice. The lysates were spun down at maximum speed, at 4 °C for 30 min. Protein A sheparose CL-4B (GE Healthcare Lifesciences) was prepared following the manufacturer's instructions and used to pre-clear the homogenates for at least 1 h, at 4 °C while tumbling. After removing the Protein A sepharose, samples were incubated with 20 μg of antibody at 4 °C overnight in a head-over-head shaker. Dysferlin IP was performed using F4 antibody, a monoclonal llama-derived antibody (kindly provided by Dr. Van der Mareel) or commercial antibodies against different dysferlin partners (mouse anti-cytoplasmic dynein (Sigma, Saint Louis, MO) or mouse anti-Trim72/MG53 (AbCam, Cambridge, UK). As a control for non-specific unions, a commercial control isotype antibody was used for dynein and trim72/MG53 IP, and a llama-derived antibody anti-β-amiloid was used as a control of isotype for the F4 antibody (kindly provided by Dr. Van der Mareel) (Huang et al., 2005). The immunocomplexes were precipitated by adding protein A sepharose incubated for at least 2 h at 4 °C while tumbling. The immunoprecipitated complexes were eluted by boiling in sample buffer 2×, and analyzed in a SDS-PAGE at 10% acrylamide treated with silver staining. The bands obtained were sequenced by MS/MS. Each experiment was performed at least twice.

Some of these results were confirmed by Western blot, transferring the proteins to a nitrocellulose membrane (Whatman, Dassel, Germany) that was blocked using the Odyssey blocking reagent (Li-COR, Lincoln, Nebraska, USA). For the immunodetection of dysferlin, the Hamlet I monoclonal antibody (Novocastra, Newcastle Upon Tyne, UK) was used and revealed using a goat-anti-mouse IR_Dye 800 (Li-COR). The membrane was visualized using the Odyssey infrared scanner (Li-COR).

Table 1
Skeletal muscle samples of patients used in this work.

Sample	Disease	Sex	Age	Mutation 1	Mutation 2
DMD1	Duchenne muscular dystrophy	Male	13	c.6439-?_7309+?del/r.(6615_7309del)/p.	X-linked
FSHD1	Fascio-scapulo-humeral dystrophy	Male	50	D4Z4 contraction 34Kb (probe p13E-11)	Autosomal dominant
Dysf1	Dysferlinopathy	Male	15	p. Arg1038X	p. Ala1064_Glu1065dup
Dysf2	Dysferlinopathy	Male	25	p.Gly1628Arg	p.Gly1628Arg

2.4. Blue native (BN)

BN experiments were performed with muscle biopsies and cultured myotubes. Samples were prepared with NativePAGE™ Sample buffer (Invitrogen, Carlsbad CA) adding 2% digitonin, obtaining a lysate with a protein:detergent ratio of 1:2. Samples were incubated on ice for 15 min and centrifuged at 20,000 × *g* for 30 min at 4 °C. Immediately prior to loading samples onto NativePAGE™ Novex Bis-Tris Gels (Invitrogen), a 5% NativePAGE™ G-250 Sample Additive (Invitrogen) was added to the samples. Next, 4–10 mg of protein extracts were run in gradient 4–12% acrylamide precast gels following the manufacturer's instructions (Invitrogen) For our BN-PAGE experiments, the concentration of blue dye was 0.02% (w/v). Electrophoresis was performed at 150 V for 1 h and a half, followed by a further 2 h at approximately 250 V. After electrophoresis, the gel was stained using the Colloidal Blue Staining Kit (Invitrogen) following the manufacturer's instructions.

Some lanes of each gel were stored at −80 °C and others were transferred to a PVDF membrane to perform a Western blot.

Non-specific binding sites were blocked with 5% skimmed milk in phosphate saline buffer (PBS). For the immunodetection, we used the monoclonal antibody Hamlet (Novocastra) for dysferlin and a rabbit monoclonal antibody to detect Trim72/MG53 (AbCam, Cambridge, UK). After washing the non-bound primary antibody, membranes were incubated with a secondary antibody goat anti-mouse or goat-anti-rabbit, conjugated with horseradish peroxidase and developed using supersignal (Thermo Fisher Scientific, Rockford, IL, USA).

After the Western blot was probed with an anti-dysferlin, the lanes stored at −80 °C were stained with colloidal blue (invitrogen) and the positive bands for dysferlin were cut for peptide sequencing with MS/MS. This experiment was performed twice.

2.5. In–gel digestion and mass spectometry analysis

The protein bands of interest were excised and trypsinized following the protocol previously described (Shevchenko et al., 2006) leaving out reduction and alkylation. Extracted peptides were analyzed on a Linear Trap Quadrupole (LTQ)-Orbitrap XL (Thermo Fisher Scientific, Rockford, IL, USA) fitted with a nanospray source (Proxeon, Thermo Fisher Scientific) previous nanoLC separation in an Agilent 1200 nano flow system (Agilent, Santa Clara, CA, USA). Peptides were separated in a reverse phase column, 100 μm × 150 mm (Nikkyo Technos Co., Ltd., Tokyo, Japan) with a gradient of 2.4–36% acetonitrile with 0.1% formaldehyde in 24 min at a flow of 0.5 μl/min. The LTQ-Orbitrap XL was operated in positive ion mode with nanospray voltage set at 2.2 kV and source temperature at 275 °C. The instrument was externally calibrated using Ultramark 1621 for the Fourier transform mass analyzer. An internal calibration was performed using the background polysiloxane ion signal at *m*/*z* 445.120025 as the calibrant. The instrument was operated in data dependent analysis mode (DDA). In all experiments full MS scans were acquired over a mass range of *m*/*z* 350–2000 with detection in the Orbitrap mass analyzer at a resolution setting of 60,000. The fragment ion spectra produced via collision induced dissociation (CID) were acquired in the LTQ mass analyzer. Following each survey, in each cycle of DDA analysis, the five most intense ions were scanned above a threshold ion count of 5000 and were selected for fragmentation at normalized collision energy of 35%. All data were acquired with Xcalibur 2.1 software. Proteins were identified using MASCOT (Matrix Science, London, UK) as search engine.

Data were processed and searched against swissprot human database. Oxidation of methionine was set as variable modifications. Peptide tolerance was 7 ppm in MS and 0.5 Da in MS/MS mode, maximum number of missed cleavages was set at 2.

2.6. Immunocytochemistry

Immunocytochemistry for the FLIM/FRET analyses was performed in control myotubes from three different subjects cultured on LabTek chamber slides (Nunc Nalge, Roskilde, Denmark) in the culture conditions indicated in the primary cultures section. Immunocytochemistry for protein localization studies was performed in myotubes from control, patients with dysferlin myopathy and a patient with Duchenne muscular dystrophy. Dysferlinopathy patients were 25 and 15 years old males. The patient with DMD was a 13 years old male (Table 1).

Cells were fixed in cold methanol for 10 min at 4 °C and blocked with Tris buffer saline supplemented with 1% bovine serum albumine (BSA), 1% normal human serum, 0.5% donkey serum and 0.01% Triton X-100.

Primary antibodies (Table 2) were incubated for 2 h at room temperature and labeled with Alexa Fluor 488 or 555 donkey secondary antibodies (Invitrogen).

2.7. Immunohistochemistry on human muscle frozen sections

For the immunohistochemistry studies we used 7 μm tissue sections from human biopsies of several patients: two 25 and 15 years old males with dysferlinopathy; a 50 years old male with fascio-scapulo-humeral dystrophy (FSHD) and 2 healthy patients (Table 1). Tissue sections were fixed in acetone for 5 min at 4 °C and blocked with Tris buffer saline supplemented with 1% BSA, 1% normal human serum, 0.5% donkey serum and 0.01% Triton X-100.

Primary antibodies (Table 2) were incubated for 2 h at room temperature and labeled with Alexa Fluor 488 or 594 donkey secondary antibodies (Invitrogen).

All pictures were acquired with a Laser Scanning Confocal Inverted Microscope Leica TCS SP5-AOBS.

2.8. Quantitative FRET efficiency through fluorescence lifetime analysis (FLIM)

FLIM–FRET is used to image direct protein–protein interactions in cells. The technique is based on the observation of fluorescence lifetime (the time of fluorophore emission after brief excitation, measured in picoseconds) of a donor fluorophore in the presence of an acceptor fluorophore. While transferring energy from an excited donor to an acceptor, FRET decreases the donor fluorescence lifetime and increases the acceptor fluorescence lifetime. Because the energy transfer is highly distance dependent, detection of FRET

Table 2
Antibodies used in this study.

Antigen	Antigen source/specificity	Antibody	Clone/ID	Company	Techniques
Dysferlin	aa 1999–2016	MoAb/mouse IgG1	Ham1/7B6	Novocastra	FLIM, WB, IHQ
Dysferlin	C-terminus	PoAb/rabbit monoclonal	ab15108	AbCam	FLIM
Dysferlin	N-terminus	PoAb/rabbit polyclonal		Genway	FLIM
F4, dysferlin	N-terminus	Llama-derived		[a]	IP
Trim72	Full length corresponding aa 1–269	MoAb/mouse plyclonal IgG	Ø	AbCam	FLIM
Trim72	aa 288–337	PoAb/rabbit IgG	Ø	AbCam	FLIM, IHQ, WB
AHNAK	N-terminus	MoAb/mouse IgG1	EM-09	AbCam	FLIM
Caveolin-3	aa 3–24	MoAb/mouse IgG1	26	BD transduction	FLIM
Dynein	Full length recombinant protein	MoAb/mouse IgG2ak	1C8	Sigma	FLIM, WB, IHQ
Annexin A1	Full length recombinant protein	PoAb/rabbit polyclonal	Ø	Invitrogen	FLIM
Myomesin2	N-terminus	PoAb/goat polyclonal	H16	Santa Cruz	FLIM
Myomesin2	N-terminus	PoAb/goat polyclonal	N20	Santa Cruz	FLIM
Calsequestrin 1	N-terminus aa 31–90	PoAb/rabbit polyclonal	H60	Santa Cruz	FLIM
Dystrophin	C-terminus	MoAb	DY4/6D3	Novocastra	FLIM
Dystrophin	aa 3661–3677	PoAb/rabbit polyclonal IgG	Ø	AbCam	FLIM

[a] Antibody kindly provided by Dr. Silvere VanDerMareel.

requires that the two fluorophores must be within ~1–10 nm, the distance typically found for directly interacting proteins (Förster et al., 1948). We used Alexa Fluor 488 as a donor and Alexa Fluor 555 as an acceptor, and we measured changes in the fluorescence lifetime of the donor.

The sample was excited using 470 nm pulsed laser with 40 MHz repetition rate and was detected using a time-correlated single photon counting detector. A fluorescence filter (500–550 nm) limited the detection of the donor fluorescence only (Alexa Flour 488). SymPhoTime software was used to measure fluorescence lifetimes on a pixel-by-pixel basis with high spatial resolution. Donor fluorophore lifetimes were fitted to two exponential decay curves to calculate the fraction of fluorophores within each pixel that either interact or do not interact with an acceptor. These lifetimes were then mapped by pseudocolor on a pixel-by-pixel basis over the entire image.

All pictures were acquired with a Laser Scanning Confocal Inverted Microscope Leica TCS SP5-AOBS, equipped with PicoQuant LSM Upgrade Kit for FLIM and FCS, which was used to perform FLIM–FRET experiments.

The following controls were used to establish and validate the FLIM assay: (A) As a negative control, Alexa Fluor 488 lifetime (dysferlin) was measured in the absence of the acceptor; (B) As a positive control, cells were immunostained for dysferlin that was visualized with two different secondary antibodies, a donkey anti-mouse Alexa Fluor 488 and a donkey anti-mouse Alexa Fluor 555; (C) In cells in which FLIM–FRET analysis was positive, we selected an area within the cell where Alexa Fluor 555 acceptor was photobleached. The resulting FLIM image showed an increase in the Alexa fluor 488 fluorescence lifetime within this area that was identical to the Alexa Fluor 488 lifetime in the absence of an acceptor; (D) The same cells were immunostained with an antibody predicted to colocalize but not interact with Dysferlin. Double immunostaining shows that Dysferlin (Alexa Fluor 488) colocalizes with Dystrophin (Alexa Fluor 555) at the sarcolemma. However, despite colocalization, Alexa Fluor 488 lifetime was the same as in the negative control (A), suggesting that Dystrophin does not interact with Dysferlin. All experiments were performed in at least 3 independent assays and on 30 different cells.

The lifetime average decay was calculated comparing the lifetime average depending on pluorophore amplitude of negative controls (only donor fluorophore) and the protein pair of interest. Each experiment was analyzed independently, as the lifetime average could change depending on many factors such as scattered light. Pseudocolored images were produced using the SynPhoTime software to represent an image of the result. However, the nature of the interaction was established according to the % of lifetime average decay and not to the pseudocolored images.

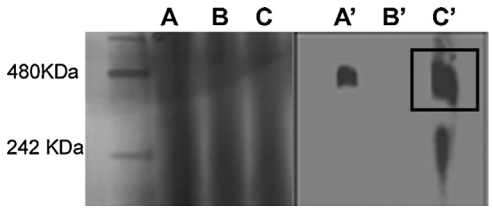

Fig. 1. Blue native and WB image showing bands for dysferlin complex and trim72/MG53 complex. Adult skeletal muscle extract from healthy patient was run in a native-PAGE gradient gel (4–12% acrylamide) in all lanes (A)–(C). Lanes (A) and (C) were immunoblotted and probed with an antibody to Trim72/MG53 (A′) or to dysferlin (C′). Lane (B) was used for MS/MS sequencing of the bands recognized by the antibodies in lanes (A′) and (C′).

2.9. Statistical analysis

Although most FLIM–FRET studies do not use statistical analysis (Badiola et al., 2011) for sake of robustness of the results, we performed comparisons of lifetimes obtained with FLIM–FRET analysis by two-way analysis of variance (ANOVA). Lifetimes average was set as the dependent variable and the day of experiment and the type of sample (only donor staining vs donor and acceptor staining) the independent variables. Statistical significance was set at $p < 0.05$.

3. Results

3.1. Dysferlin complex analysis

Blue native electrophoresis technique is used to detect protein complexes because the protein extracts are prepared with low detergent concentrations that do not disturb protein complexes and consequently protein–protein interactions. BN analysis of human skeletal muscle from muscle biopsies combined with WB, revealed 2 bands that were positive with anti-dysferlin antibodies (Fig. 1). We used the same extract to perform a WB using an anti-tim72/MG53 antibody (Fig. 1), where we detected a single band corresponding to the heaviest band observed on the WB probed with an anti-dysferlin antibody. This heaviest band was selected for mass spectrometry studies. In parallel, we performed IP assays using adult skeletal muscle and human myotube extracts to asses these results (Fig. 2), as other proteins or protein complexes could be present at the same molecular weight as our complex of interest.

Each BN and IP experiment was performed at least twice. To obtain a reliable list of proteins corresponding to the dysferlin complex we matched the mass spectrometry results from the heaviest band on BN experiments with IP experiments both in adult skeletal muscle tissue and myotubes. To the final list of proteins we included only those detected in more than one experiment. All proteins listed had a mascot score ≥30. Finally, we compared our list with published data (Table 3).

Table 3
Proteins identified as members of the dysferlin complex by IP and BN.

Accession	Description	MW [kDa]	BN	Score	Coverage	Sample	IP	Score	Coverage	Sample	Bibliography
P08237	6-Phosphofructokinase, muscle type	8,512,839	+	403,401	40	asm	+	7,297,265	33.08	mt	1
P24752	Acetyl-CoA acetyltransferase, mitochondrial	4,517,065	+	8,857,457	7.03	asm	+	5,464,835	37.94	mt	
P68133	Actin, alpha skeletal muscle	4,202,385	+	7,721,488	52.25	asm	+	6,500,666	62.07	mt	
P61158	Actin-related protein 3	47.37	–	–	–	–	+	4,498,307	32.78	asm	1
Q86TX2	Acyl-coenzyme A thioesterase 1	4,624,806	+	59.13	6.65	asm	+	1,783,144	9.5	mt	
P30566	Adenylosuccinate lyase	5,485,397	+	3,383,361	25.83	asm	+	9,524,954	3.51	mt	1
P61163	Alpha-centractin	4,258,691	–	–	–	–	+	1,241,169	9.04	asm, mt	
P08758	Annexin A2	3,857,982	+	9,813,443	26.55	asm	–	–	–	–	1, 2, 3
P08758	Annexin A5	359,144	+	1,813,043	28.75	asm	+	56.51	4.69	mt	
P17174	Aspartate aminotransferase, cytoplasmic	4,621,853	+	24,615	21.07	asm	+	381,899	30.02	mt	
P13929	Beta-enolase	4,690,228	+	8,961,892	35.94	asm	+	445,269	29.95	asm	1
P55287	Cadherin-11	87	–	–	–	–	+	68	31.5	mt	
O75746	Calcium-binding mitochondrial carrier protein Aralar1	7,471,485	+	8,762,516	9.14	asm	+	241	7.67	asm	1
P17655	Calpain-2 catalytic subunit	7,995,881	+	57.44	2.14	asm	+	1,237,321	5.43	mt	1
P20807	Calpain-3	94.2	+	–	1.22	–	–	–	–	–	4
P31415	Calsequestrin-1	4,447,064	+	5,084,371	22.31	asm	–	1,105,063	13.33	mt	
O14958	Calsequestrin-2	464,068	+	48.72	6.77	asm	+	4,792,158	31.08	asm	
P12277	Creatine kinase B-type	4,261,732	+	9,306,455	19.95	asm	+	1,228,625	7.09	mt	1
P06732	Creatine kinase M-type	430,739	+	1,550,346	52.23	asm	+	4,722,021	54.07	asm, mt	1
P17540	Creatine kinase S-type, mitochondrial	4,747,436	+	7,071,174	36.04	asm	+	1,989,533	14.8	mt	
O43237	Cytoplasmic dynein 1 light intermediate chain 2	54	–	–	–	–	+	1,123,511	18.81	asm	1, 3
O75923	Desmin	5,350,315	+	37.33	3.83	asm	+	4,558,238	28.3	mt	1
O75923	Dysferlin	2,371,442	+	1,291,806	2.4	asm	+	4,174,846	8.51	asm, mt	
P21333	Filamin-A	2,805,639	+	465,118	1.55	asm	+	6,638,752	1.44	asm	1
Q14315	Filamin-C	2,908,406	+	1,001,729	24.81	asm	+	2,949,599	2.64	mt	1
Q13642	Four and a half LIM domains protein 1	3,623,865	+	1,511,605	15.48	asm	+	62.52	3.72	mt	1
P04075	Fructose-bisphosphate aldolase A	3,939,531	+	8,005,569	48.08	asm	+	5,697,502	38.74	mt	1
P04406	Glyceraldehyde-3-phosphate dehydrogenase	360,304	+	1,122,799	52.24	asm	+	2,611,433	23.28	mt	
Q14974	Importin subunit beta-1	9,710,802	+	1,729,755	2.85	asm	+	72.08	1.83	asm	
P48735	Isocitrate dehydrogenase [NADP], mitochondrial	5,087,687	+	6,144,867	32.08	asm	–	617,111	35.18	mt	
P54296	Myomesin-2	1,647,924	+	1,013,329	17.06	asm	+	77	54.68	asm	
P35580	Myosin-10	228,858	+	7,823,054	1.77	asm	+	6,701,318	45.29	asm, mt	
P11055	Myosin-3	2,237,665	+	2,644,128	22.58	asm	+	4,351,744	41.86	asm, mt	
P35579	Myosin-9	2,263,916	+	328,331	5.46	asm	+	3,654,077	63.98	asm, mt	
Q09666	Neuroblast differentiation-associated protein AHNAK	6,286,994	+	6,681,776	7.52	asm	–	–	–	–	1, 5
P14618	Pyruvate kinase isozymes M1/M2	5,790,003	+	1,652,692	40.49	asm	+	310	67.81	mt	1
P00558	Phosphoglycerate kinase 1	4,458,613	+	2,182,857	29.98	asm	+	7,807,532	50.84	mt	1, 3
Q6NZI2	Polymerase I and transcript release factor (PTRF)	4,344,982	+	1,900,171	14.62	asm	–	–	–	–	1, 6
Q13885	Protein S100-A1	1,053,914	+	7,311,375	22.34	asm	–	–	–	–	3
P68371	Ryanodine receptor 1	564,815	+	1,376,783	1.09	asm	–	–	6.53	–	1
Q13509	Sarcoplasmic/endoplasmic reticulum calcium ATPase 1	1,101,816	+	8,860,698	32.47	asm	+	3,926,444	14.79	asm, mt	1
P08670	Stress-70 protein, mitochondrial	7,363,478	+	1,676,971	2.36	asm	+	46	–	mt	
P54296	Tripartite motif-containing protein 72	5,269,704	+	5,598,927	42.56	asm	+	2,064,456	10.9	asm	1, 7
Q09666	Tubulin beta chain	4,963,897	+	5,011,932	38.96	asm	+	1,825,154	32.21	asm, mt	8
P18206	Tubulin beta-2A chain	4,987,496	+	5,699,422	37.98	asm	+	1,736,265	51.69	asm	
P54296	Tubulin beta-2C chain	49,799	+	7,171,555	51.48	asm	+	1,737,109	33.26	asm	
O75746	Tubulin beta-3 chain	5,040,026	+	4,358,945	26.89	asm	+	1,517,186	20.22	asm	
P23297	Tubulin beta-4 chain	495,539	+	439,277	44.37	asm	+	1,458,786	25	asm	
P31415	Tubulin beta-6 chain	49,825	+	265,243	18.61	asm	+	1,702,747	33.63	asm	1, 3
O14958	Vimentin	5,361,908	+	4,376,831	4.08	asm	+	147,263	8.58	asm, mt	1
P21817	Vinculin isoform 1	1166	+	295	1.85	asm	–	–	–	–	

(1) de Morree et al. (2010); (2) Lennon et al. (2003); (3) studies Campanaro et al. (2002); (4) Huang et al. (2007); (5) Huang et al. (2008); (6) Cacciottolo et al. (2010); (7) Cai et al. (2009b); (8) Azakir et al. (2010).

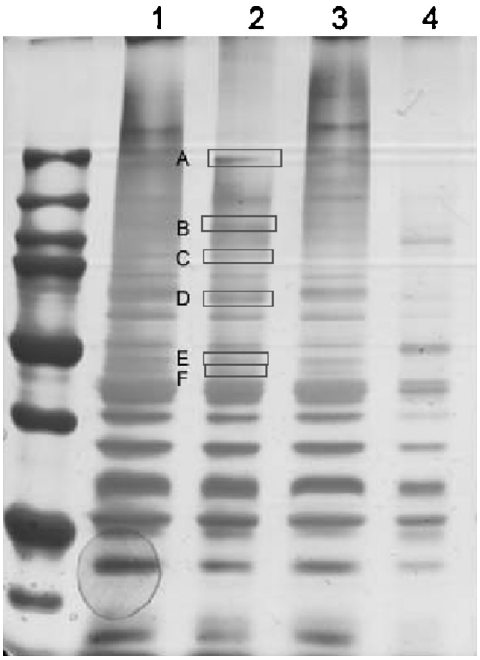

Fig. 2. Silver stain of IP extracts separated in a SDS-PAGE gel. Lane 2 shows the proteins immunoprecipitated using the monoclonal antibody to dysferlin F4 from human myotubes protein extract. Lane 1 shows the supernatant from the same experiment. Lane 4 shows the proteins immunoprecipitated using a monoclonal llama-derived antibody used as a control of isotype in human myotubes. Lane 3 shows the supernanant from the same experiment. Bands A, B, C, D, E and F were sequenced by MS/MS. Band A corresponds to myosins 3, 9 and 10; Band B corresponds to cadherin-11; band C and corresponds to Cytoplasmic dynein 1 intermediate chain 2; Band D corresponds to Pyruvate kinase isozymes M1/M2; band E corresponds to Trim72/MG53 and band F corresponds to vimentin and tubulin beta chain.

Some proteins detected by both IP and BN were selected for FLIM–FRET analysis to confirm the type of interaction between them and dysferlin.

As expected, the positive control for FLIM–FRET analysis of dysferlin using two different secondary antibodies showed a decrease in Alexa fluor 488 fluorescence lifetime in presence of Alexa Fluor 555 (9.32%, maximum decay from 2.3 ns to 1.4 ns, Fig. 3B).

3.2. Trim72/MG53 and AHNAK interact directly with dysferlin

Trim72/MG53 was found in the dysferlin complex by BN and was co-immunoprecipitated with dysferlin in adult skeletal muscle extract (Fig. 2 band E). AHNAK was also found within the dysferlin complex by BN using adult skeletal muscle extracts.

To assess whether their interaction was direct or indirect we performed FLIM–FRET analysis. We observed a lifetime average decay of 2.86% ($p < 0.05$) for the dysferlin–Trim72/MG53 protein pair. The donor fluorophore (Alexa Fluor 488, dysferlin) had a fluorescence lifetime average of ~3.2 ns in the absence of a FRET acceptor. In cell areas where the acceptor (Alexa Fluor 555, Trim72/MG53) was close to the donor (blue pixels in the pseudo-colored image, Fig. 3), the lifetime was shortened to ~2.5 ns (Figs. 3 and 4) indicating interaction between both proteins on those sites. When we studied this interaction in injured cells, we could not observe differences as the lifetime average decay was 2.66% ($p < 0.05$) (Figs. 3F and 4).

When we studied dysferlin–AHNAK interaction by FLIM–FRET analysis, the lifetime average decay was 4.01% ($p < 0.05$), showing a direct interaction between these two proteins (Figs. 3H and 4). The maximum lifetime decay was from 2.4 ns to 1.3 ns.

These findings were further confirmed by using a positive control for FLIM–FRET analysis – dysferlin–annexin-A1 protein pair, an already known interaction (Lennon et al., 2003) – obtaining a lifetime average decay of approx 8.95% ($p < 0.05$) (Figs. 3K and 4). As a negative control, we performed FLIM–FRET analysis of the dysferlin–dystrophin pair. No interaction was observed, as expected from the bibliography (Piccolo et al., 2000) as the lifetime average decay was about 0.46% ($p = 0.19$) (Figs. 3I and 4) and scattered blue pixels were observed in the pseudo-colored image.

3.3. Caveolin-3 does not interact directly with dysferlin

It has been reported that dysferlin and caveolin-3 co-immunoprecipitated (Matsuda et al., 2001). In our experiments, Cav-3 was found in the dysferlin complex by BN. To avoid a possible artifact due to the molecular distance between the antibodies used to detect dysferlin and caveolin-3, we designed two experiments. We performed FLIM–FRET analysis with a monoclonal antibody against caveolin-3, which binds the N-terminus of the protein. Dysferlin was labeled either with a rabbit monoclonal antibody directed to the N-terminus, or with a polyclonal antibody that recognizes the C-terminus of the protein. Neither of these experiments showed lifetime decay (0.18%) (Figs. 3L and 4), indicating that this interaction is not direct.

Our experiments and those of other authors (Cai et al., 2009b) show that caveolin-3 forms a complex with dysferlin and Trim72/MG53. Also, as described above, we found that the interaction of caveolin-3 and dysferlin is not direct. These findings prompted us to study whether the interaction of caveolin-3 with dysferlin requires the binding of Trim72/MG53 to both proteins. Interestingly, FLIM–FRET analysis showed a direct interaction between caveolin-3 and Trim72/MG53 as it showed a lifetime average decay of 2.56% ($p < 0.05$) (Suppl. Fig. 1).

Supplementary data associated with this article can be found, in the online version, at http://dx.doi.org/10.1016/j.biocel.2013.06.007.

3.4. Myomesin-2, calsequestrin-1 and cytoplasmic dynein display a direct interaction with dysferlin

Calsequestrin-1 and myomesin-2 were found by BN and IP in adult skeletal muscle. We also found different subunits of the cytoplasmic dynein in the dysferlin complex by BN in adult skeletal muscle. Cytoplasmic dynein was also found by IP of dysferlin both in adult skeletal muscle and myotubes.

To further analyze the interaction of these proteins with dysferlin we performed FLIM–FRET analysis. The lifetime average decay for the dysferlin–calsequestrin-1 protein pair was 3.58% ($p < 0.05$), showing direct interaction between those two proteins (Figs. 3C and 4). The maximum lifetime decay was from 2.3 ns to 1.4 ns.

The lifetime average decay for dysferlin–myomesin-2 protein pair was 3.68% ($p < 0.05$), showing direct interaction between these two proteins (Figs. 3N and 4). The maximum lifetime decay was from 2.3 ns to 1.4 ns.

The FLIM–FRET analysis of the dysferlin–dynein interaction was performed using an antibody against the cytoplasmic dynein 1 light intermediate chain 2 (DYNC1LI2), that was the most frequently detected subunit in our IP and BN experiments. The lifetime average decay for this protein pair was 2.76% ($p < 0.05$). The maximum lifetime decay was from 2.1 ns to 1.3 ns that was recovered in a given region of interest after photobleaching (Figs. 3O and 4), confirming the interaction.

3.5. Immunolocalization studies on muscle biopsies and human myotubes

We studied the expression pattern of all the proteins analyzed using FLIM–FRET analysis in muscle biopsies and human myotubes from controls, patients with dysferlinopathy and patients with other muscular dystrophies. Staining with Trim72/MG53 in muscle biopsies showed accumulation of the protein in patches at the sarcolemma that were more abundant in patients with dysferlinopathy than in those with fascio-scapulo-humeral dystrophy (FSHD). Furthermore, staining of the sarcoplasm was weaker in patients with dysferlinopathy (Fig. 5H). Similar results were observed in a previous study (Waddell et al., 2011). In myotubes from patients with dysferlinopathy we observed aggregates of Trim72/MG53 in the sarcoplasm (Fig. 6H). Trim72/MG53 is slightly more expressed in DMD myotubes than in controls but do not form the aggregates observed in dysferlin-deficient myotubes. Immunohistochemistry for dynein also showed a different pattern in the muscle biopsies of patients with dysferlinopathy. The protein accumulated at the subsarcolemma and was reduced at the sarcoplasm (Fig. 5E). Dynein was expressed mainly in fast fibers although some staining is also observed in slow fibers (Suppl. Fig. 2). Dynein accumulated around the nuclei in myotubes from patients with dysferlinopathy (Fig. 6E) and showed a diffuse staining of the sarcoplasm in control (Fig. 5D) and Duchenne muscular dystrophy (DMD) samples (Fig. 6F).

Supplementary data associated with this article can be found, in the online version, at http://dx.doi.org/10.1016/j.biocel.2013.06.007.

Calsequestrin-1 expression in human biopsies was similar in control, dysferlin-deficient and FSHD samples (data not shown), and in human myotubes from dysferlin-deficient and DMD patients (Fig. 6K and L).

Expression of AHNAK, caveolin-3 and myomesin-2 was similar in all samples studied, except for annexin A1 where we observed an increased expression forming small cytoplasmatic aggregates (Suppl. Fig. 3). In fact, increased expression of annexin A1 has been reported in several muscular dystrophies and the authors suggest that the expression seems to correlate with the degree of muscle degeneration (Cagliani et al., 2005).

Supplementary data associated with this article can be found, in the online version, at http://dx.doi.org/10.1016/j.biocel.2013.06.007.

4. Discussion

Our results show that the combination of IP, BN, and FLIM–FRET is more informative and reliable to study the composition and interactions of proteins within a complex than a single technique. IP is extensively used to determine protein–protein interactions but

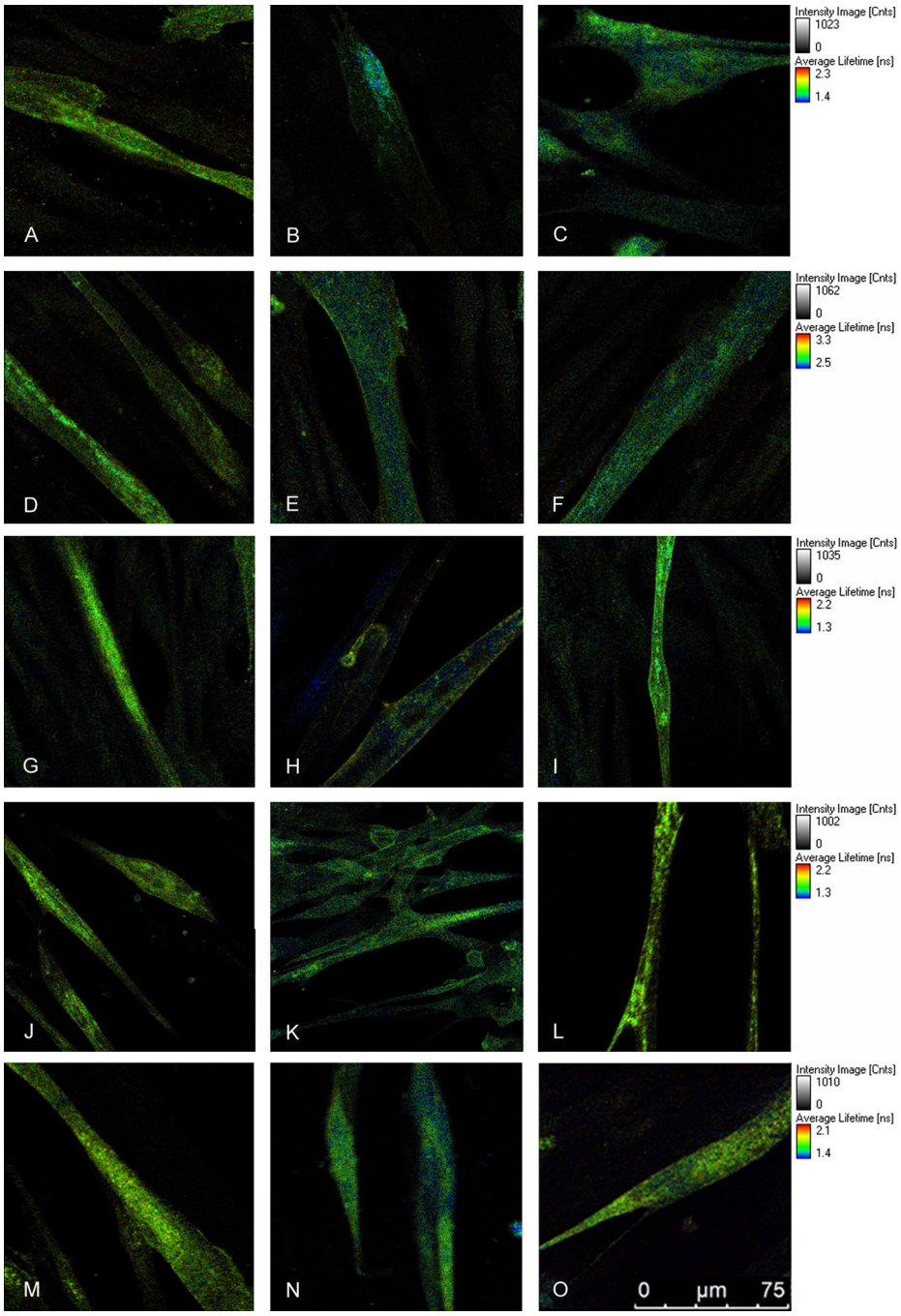

Fig. 3. FLIM analysis in human control myotubes. (A), (D), (G), (J) and (M) show donor fluorophore lifetimes in the absence of acceptor for each experiment. Only proteins closer than 10 nm show lifetime shortening (blue pixels) in the pseudo-colored images. Colorimetric scale shows alexa fluor 488 fluorophore lifetime in nanoseconds. Intensity scale represents the number of counted photons/pixel that was set at 1000 in all images. (B) Positive control with 2 different antibodies detecting dysferlin; (C) Calsequestrin-1/dysferlin interaction; (E) Trim72/dysferlin interaction in non injured cells; (F) Trim 72/dysferlin interaction in injured cells; (H) AHNAK/dysferlin interaction; (I) Dystrophin/dysferlin interaction; (K) Annexin A1/dysferlin interaction (L) Caveolin-3/dysferlin interaction; (N) Myomesin-2/dysferlin interaction and (O) Dynein/dysferlin interaction. (For interpretation of the references to color in figure legend, the reader is referred to the web version of the article.)

it has limitations such as pulling down proteins that bind non-specifically to the antibodies. BN-PAGE allows us to study protein complexes, but several complexes can be found at the same molecular weight. MS/MS analysis thus detects many proteins that are not part of our complex of interest. Although IP and BN are useful to identify proteins within a complex, techniques such as the FLIM–FRET analysis are needed to determine whether interactions within a complex are direct or indirect. Further knowledge about the interactions of proteins within a complex would help us understand their role in cell physiology.

Our study also shows that FLIM–FRET analysis can be performed in human myotubes in native conditions, avoiding the use of cell models that overexpress the proteins of interest. Although the use of vectors encoding for specific proteins tagged with GFP and RFP can be very informative, this approach does not represent a real situation since the overexpression of two proteins in a cell system can lead to non-specific interactions or bias the system toward a single interaction.

The robustness of our strategy is validated by the fact that some of the partners of dysferlin found in our study, such as AHNAK, PTRF,

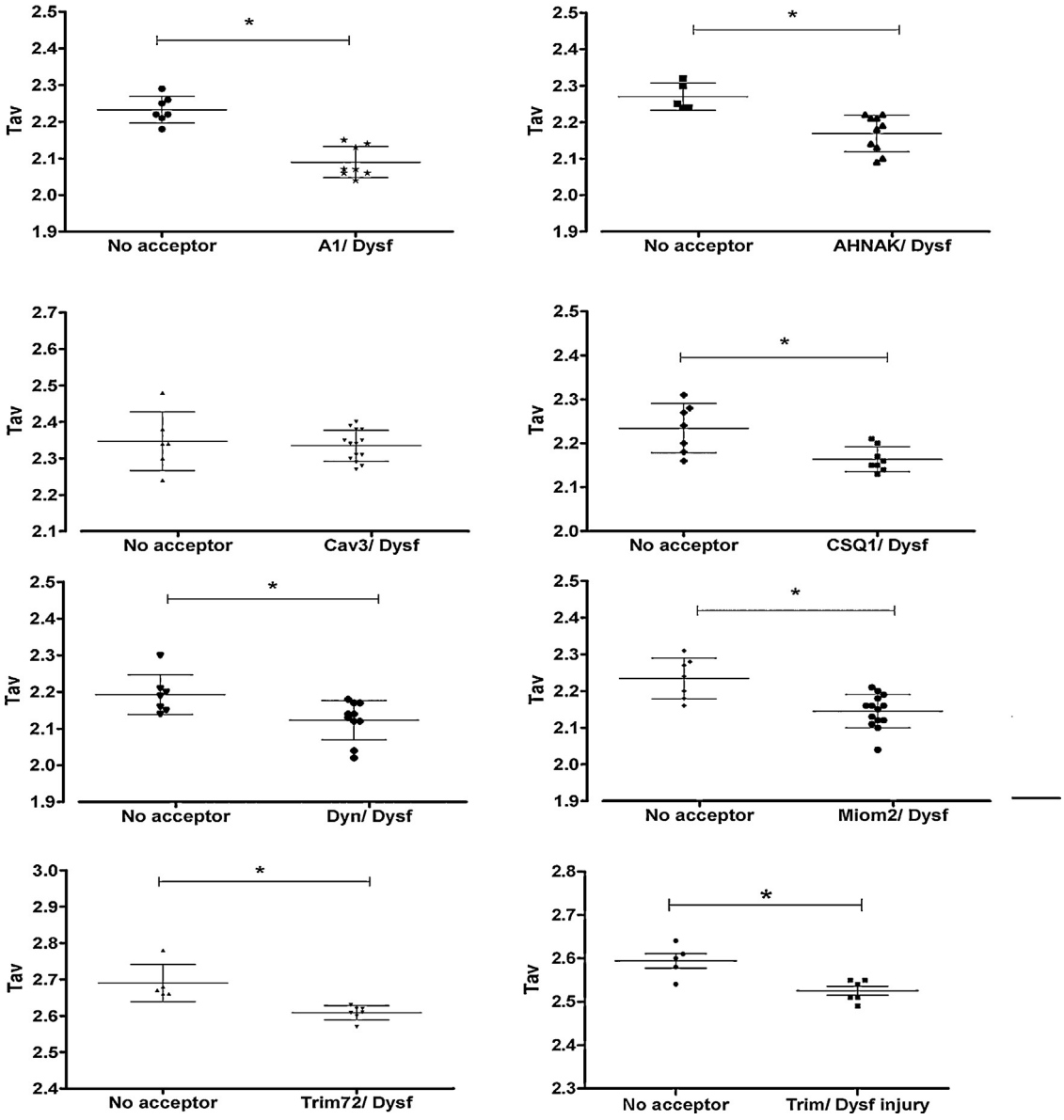

Fig. 4. FLIM–FRET analysis. Graphical representation of lifetime average (Tav) of all protein pairs studied by FLIM–FRET analysis compared to their controls with no acceptor. *<0.05.

Trim72/MG53 or Vinculin, have already been described in the literature (Huang et al., 2007; Cacciottolo et al., 2010; Cai et al., 2009b; de Morree et al., 2010). The FLIM–FRET technology allowed us to study some of those previously reported interactions in more detail. We observed a direct interaction of dysferlin and trim72/MG53 in injured and non-injured cells, suggesting that these two proteins interact before and during the repair process. Dysferlin-deficient myotubes show an abnormal distribution of Trim72/MG53. This protein has been related to membrane repair. Dystrophin deficient muscle is also more prone to injury so it is not surprising to observe a distribution of the protein different from that in controls. In DMD myotubes Trim72/MG53 seems to be more expressed than in controls but do not form the aggregates observed in dysferlin-deficient myotubes, probably because these cells express normal levels of dysferlin.

Although the lifetime decay values in our experiments were not high, they were statistically significant. These values could have been low because we used antibodies rather than labeled recombinant proteins to perform the FLIM–FRET analysis. The FLIM–FRET technique shows a positive interaction between two molecules if they are less than 10 nm apart. The use of primary and secondary antibodies adds molecular distance between the two proteins under study (Ban et al., 1994). Although this effect can be minimized using tagged recombinant proteins, all our experiments were conducted using human skeletal muscle primary cultures where proteins are present in their native form and consequently, the results reflect a more realistic situation. In another hand, the use of antibodies to perform FLIM–FRET studies allow us to stain proteins in different domains, making possible to avoid false negative results. As an example of this situation, we labeled dysferlin with two different antibodies to test its interaction with caveolin-3, because according to previous reports those two proteins interact (Matsuda et al., 2001). Our results suggest that although caveolin-3 is part of the dysferlin complex, it binds to trim72/MG53 which in turn interacts directly with dysferlin. Our strategy (IP + BN + FLIM–FRET) allowed us to find new members of the dysferlin complex such as calsequestrin-1, myomesin-2, and cytoplasmic dynein. Their interaction with dysferlin has not been

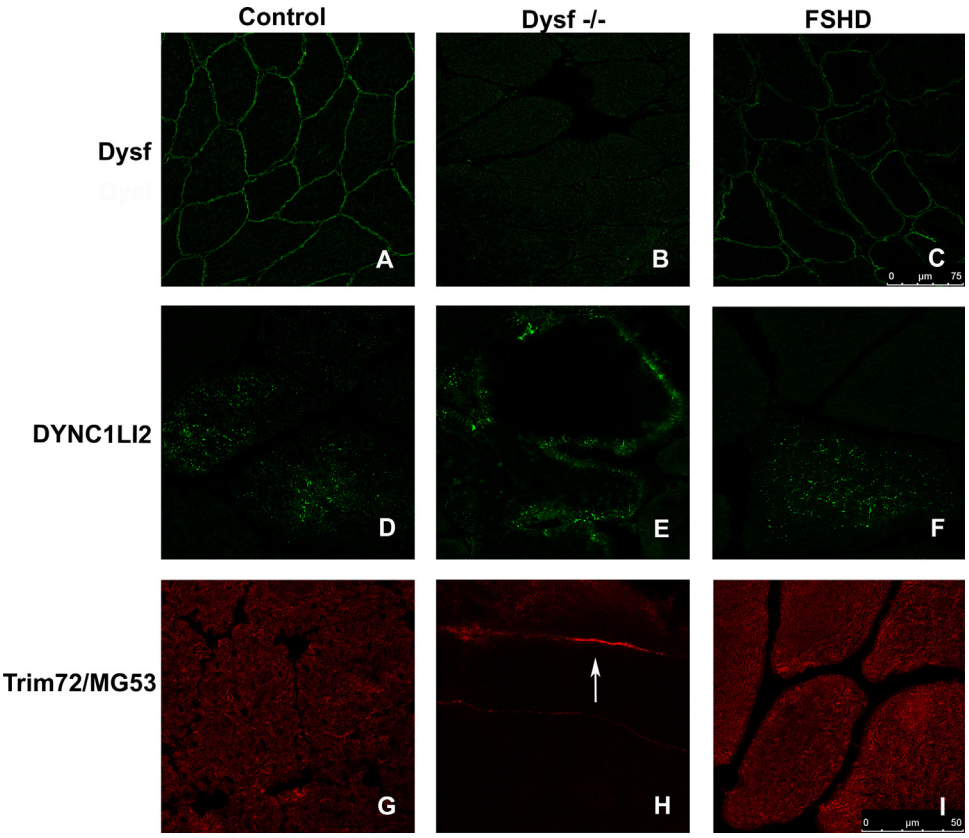

Fig. 5. Immunohistochemistry on human biopsies. Immunohistochemistry showed normal dysferlin expression pattern in a healthy control (A) and a FHSD patient (C) and absence of dysferlin in a patient with limb girdle muscular dystrophy 2B (B); Picture (D) shows the normal expression pattern of dynein (DYN) in a control muscle biopsy. In muscle sections of dysferlinopathy patients, we observe that absence of dysferlin causes accumulation of dynein at the subsarcolemma (E) that was not observed in FHSD patients (F); Trim72/MG53 expression pattern in healthy muscle is showed in picture G. We observe patches of Trim72/MG53 at the sarcolemma in patients with dysferlinopathy (H), which were occasionally observed in FHSD patients (I). Pictures (A)–(C) were taken at 630×, pictures D-I were taken at 630× with a digital zoom of 2×.

analyzed to date although they have been cited amid a list of genes and/or proteins in other studies (Campanaro et al., 2002; de Morree et al., 2010).

Calsequestrin-1 is a calcium storage protein located in the lumen of sarcoplasmic reticulum (SR) that acts as a buffering protein helping sarcoplasmic/endoplasmic reticulum calcium ATPase (SERCA) in calcium uptake (Murphy et al., 2009; Royer and Rios, 2009). Calsequestrin does not contain a transmembrane domain, and is believed to be located within the lumen of the SR (Fliegel et al., 1987), although a domain of the protein binds to the junctional face of SR membrane (Collins et al., 1990). Dysferlin is expressed in the t-tubule system (Klinge et al., 2010; Roche et al., 2011), which forms a triad with the SR. As we found a direct interaction between dysferlin and calsequestrin-1, our results suggest that dysferlin is also expressed in the SR. As dysferlin is a Ca^{2+} sensor (Therrien et al., 2009; Davis et al., 2002), it could also have a role in calcium reuptake by the SR.

Myomesin-2 also interacts directly with dysferlin. Brule et al. (2010) found that myomesin 2 co-immunoprecipitates with Calpain-3, another protein related to the dysferlin complex. Myomesin-2 is a member of the MYOM family, mainly expressed in fast fibers (Agarkova et al., 2004). The MYOM family of proteins are components of the M-band, and act as crosslinkers of myosin filaments (Agarkova et al., 2003; Agarkova and Perriard, 2005) to give stability to the sarcomere. Dysferlin has been suggested to have a role in cell membrane stability by other authors as it is related to integrins through vinculin and affixin (Matsuda et al., 2005; de Morree et al., 2010). The dysferlin/myomesin-2 interaction, suggests that dysferlin participates not only in the integrity of the sarcolemma but also in myofibril stability.

We also found that cytoplasmic dynein interacts directly with dysferlin. We also observed an abnormal distribution of dynein expression in the muscle biopsies of patients with dysferlin myopathy. Dynein is a motor protein related to retrograde vesicle transport along the microtubules (Vale, 2003). It is also involved in microtubule elongation, being responsible for the anterograde transport of short microtubules to the growing ends (Ahmad et al., 2006). Microtubules are formed by monomers of alpha-tubulin. Acetylation of alpha-tubulin leads to recruitment of cytoplasmic dynein to microtubules, enhancing vesicle transport (Dompierre et al., 2007). Cytoplasmic dynein has been previously co-immunoprecipitate with dysferlin in adult skeletal muscle and myotubes by De Morrée et al. (de Morree et al., 2010). They found that some of the proteins interacting with dysferlin participate in several vesicle transport pathways, the most relevant being endocytosis. Our results indicate that dysferlin participates in retrograde cellular transport as suggested by de Morree et al. (2010) using in silico analysis. In addition, Demonbreun et al. (2010) described that dysferlin-null myoblasts have a defect in the endocytic receptor recycling compartment (RRC). This underlines the function of dysferlin in vesicle trafficking and endocytic recycling. In agreement with this hypothesis it has recently been reported that dysferlin regulates the acetylation state of alpha-tubulin (Di Fulvio et al., 2011). In dysf-null myoblasts, the acetylation state of alpha-tubulin is reduced. This reduction of the acetylation state of alpha-tubulin diminishes the recruitment of cytoplasmic dynein to microtubules which in turn attenuates the retrograde pathway and microtubule elongation (Dompierre et al., 2007). Finally, it has also been reported that dynein inhibitors interfere with the reorientation of the microtubule cytoskeleton during healing of

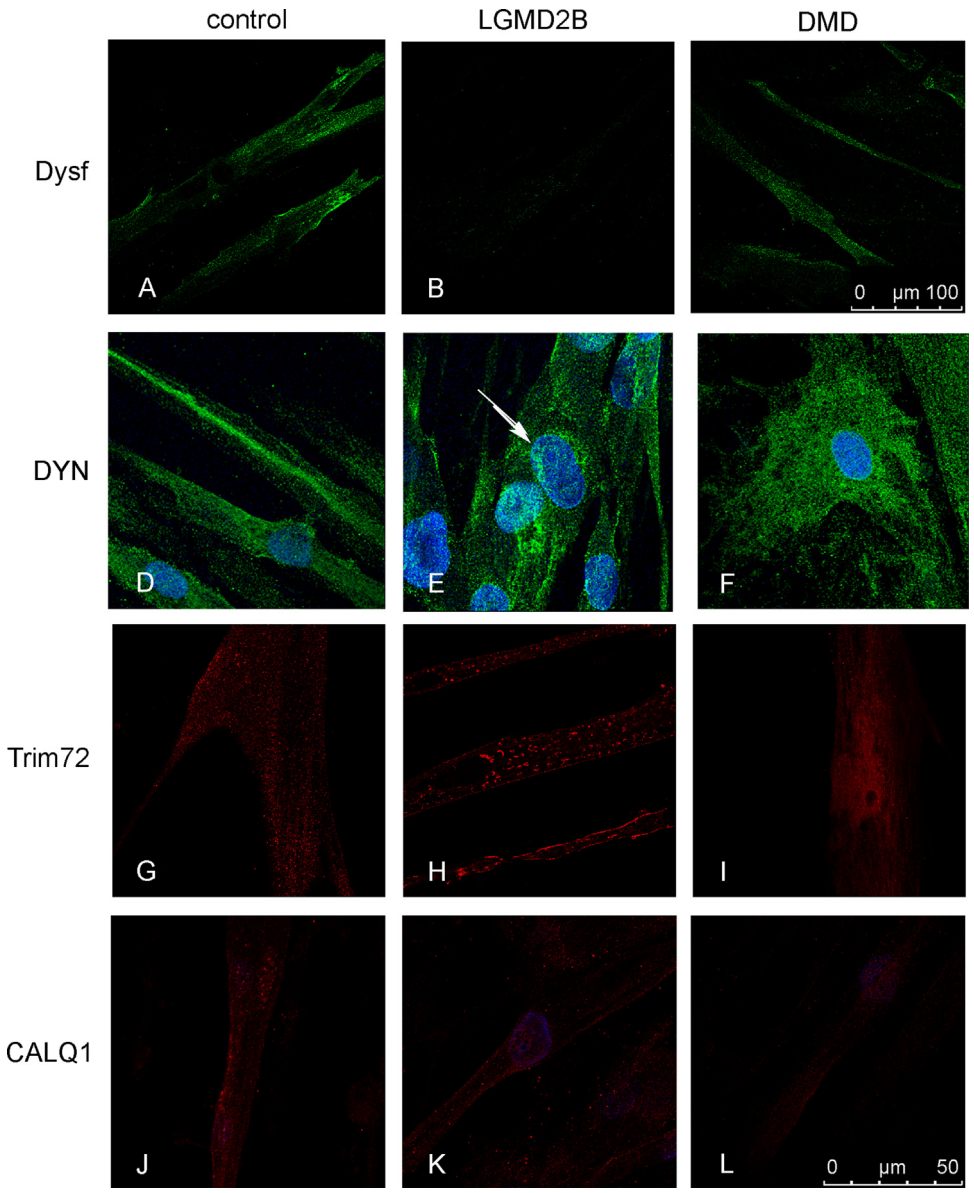

Fig. 6. Immunocytochemistry in human myotubes. Immunocytochemistry showed normal dysferlin expression in control myotubes (A) and myotubes from a DMD patient (C) and absence of dysferlin in myotubes from a patient with LGMD2B (B); Picture (D) shows normal expression pattern of dynein (DYN) in control myotubes. In myotubes from dysferlinopathy patients, we observe that the absence of dysferlin causes an accumulation of dynein around nuclei (E, arrow) that was not observed in DMD myotubes (F); Trim72/MG53 expression pattern in control myotubes is showed in (G). Absence of dysferlin causes accumulation of Trim72/MG53 in dysferlinopathy patients (H), which is not observe in myotubes from DMD patients (I). Normal expression of Calsequestrin-1. (CALQ1) in control myotubes (J), seems to be reduced in dysferlinopathy (K) and DMD patients (L). Pictures (A)–(L) were taken at 630×, with a digital zoom of 2.5×. Arrow in panel (E) shows perinuclear accumulation of cytoplasmic dynein.

wounded NIH3T3 cells (Dujardin et al., 2003). These results are in accordance with a possible role of cytoplasmic dynein in membrane resealing, reinforcing its interaction with dysferlin. All these data furnish evidence of a role of dysferlin in cytoskeleton remodeling and stability, and sarcolemmal integrity.

Here, we propose new roles for dysferlin, as calcium signaling in the SR, myofibril stability and retrograde vesicular transport. The fact that sarcolemma repair is not the only function of dysferlin is supported by the findings that an over-expression of myoferlin can rescue dysferlin function in membrane resealing, but muscles still display a dystrophic phenotype, suggesting other important roles for dysferlin in muscle (Albrecht et al., 2010).

It is important to know which proteins interact with dysferlin as they may be mutated in other muscular dystrophies. For example, the mg53−/− mouse model shows skeletal muscle pathology, present in the form of muscular weakness and histology with an increased number of central nuclei and a reduced fiber size (Cai et al., 2009a). It has also been reported that dysferlin was abnormally expressed in a patient with Samaritan myopathy, a disorder caused by homozygous mutations in the RYR1 gene (Bohm et al., 2012). We found RYR1 in the dysferlin complex in some experiments performed in adult skeletal muscle.

5. Conclusions

Our data enlarge on previous findings suggesting that membrane resealing is not the only function of dysferlin, and that this protein probably has multiple roles in skeletal muscle physiology. We found that caveolin-3 does not interact directly with dysferlin, and MG53 probably links both proteins within the complex. It may be useful to characterize dysferlin partners to understand not only other dysferlin functions, but also the phenotypic variability

observed in dysferlinopathy patients. Such characterization may help us identify new genes involved in other muscular dystrophies where the responsible gene is unknown.

Acknowledgements

This work was supported by grants from "Fundación Isabel Gemio" and "Ministerio de Sanidad del Gobierno de España" (FIS 09/1944). We thank Carolyn Newey for editorial support and Ignasi Gich for advice in the statistical analysis.

References

Agarkova I, Perriard JC. The M-band: an elastic web that crosslinks thick filaments in the center of the sarcomere. Trends in Cell Biology 2005;15:477–85.

Agarkova I, Ehler E, Lange S, Schoenauer R, Perriard JC. M-band: a safeguard for sarcomere stability? Journal of Muscle Research and Cell Motility 2003;24:191–203.

Agarkova I, Schoenauer R, Ehler E, Carlsson L, Carlsson E, Thornell LE, Perriard JC. The molecular composition of the sarcomeric M-band correlates with muscle fiber type. European Journal of Cell Biology 2004;83:193–204.

Ahmad FJ, He Y, Myers KA, Hasaka TP, Francis F, Black MM, Baas PW. Effects of dynactin disruption and dynein depletion on axonal microtubules. Traffic 2006;7:524–37.

Albrecht DE, Garg N, Rufibach LE, Williams BA, Monnier N, Hwang E, Mittal P. 4th Annual Dysferlin Conference 11–14 September 2010, Washington, USA. Neuromuscular Disorders: NMD 2010;21:304–10.

Ampong BN, Imamura M, Matsumiya T, Yoshida M, Takeda S. Intracellular localization of dysferlin and its association with the dihydropyridine receptor. Acta Myologica 2005;24:134–44.

Askanas V, Shafiq SA, Milhorat AT. Normal and dystrophic chicken muscle at successive stages in tissue culture. Archives of Neurology 1971;24:259–65.

Azakir BA, Di Fulvio S, Therrien C, Sinnreich M. Dysferlin interacts with tubulin and microtubules in mouse skeletal muscle. PLoS ONE 2010;5:e10122.

Badiola N, de Oliveira RM, Herrera F, Guardia-Laguarta C, Goncalves SA, Pera M, Suarez-Calvet M, Clarimon J, Outeiro TF, Lleo A. Tau enhances alpha-synuclein aggregation and toxicity in cellular models of synucleinopathy. PLoS ONE 2011;6:e26609.

Ban N, Escobar C, Garcia R, Hasel K, Day J, Greenwood A, McPherson A. Crystal structure of an idiotype-anti-idiotype Fab complex. Proceedings of the National Academy of Sciences of the United States of America 1994;91:1604–8.

Bansal D, Campbell KP. Dysferlin and the plasma membrane repair in muscular dystrophy. Trends in Cell Biology 2004;14:206–13.

Bashir R, Keers S, Strachan T, Passos-Bueno R, Zatz M, Weissenbach J, Le Paslier D, Meisler M, Bushby K. Genetic and physical mapping at the limb-girdle muscular dystrophy locus (LGMD2B) on chromosome 2p. Genomics 1996;33:46–52.

Bashir R, Britton S, Strachan T, Keers S, Vafiadaki E, Lako M, Richard I, Marchand S, Bourg N, Argov Z, Sadeh M, Mahjneh I, Marconi G, Passos-Bueno MR, Moreira Ede S, Zatz M, Beckmann JS, Bushby K. A gene related to *Caenorhabditis elegans* spermatogenesis factor fer-1 is mutated in limb-girdle muscular dystrophy type 2B. Nature Genetics 1998;20:37–42.

Bohm J, Leshinsky-Silver E, Vassilopoulos S, Le Gras S, Lerman-Sagie T, Ginzberg M, Jost B, Lev D, Laporte J. Samaritan myopathy, an ultimately benign congenital myopathy, is caused by a RYR1 mutation. Acta Neuropathologica 2012;124:575–81.

Borgonovo B, Cocucci E, Racchetti G, Podini P, Bachi A, Meldolesi J. Regulated exocytosis: a novel, widely expressed system. Nature Cell Biology 2002;4:955–62.

Brule C, Dargelos E, Diallo R, Listrat A, Bechet D, Cottin P, Poussard S. Proteomic study of calpain interacting proteins during skeletal muscle aging. Biochimie 2010;92:1923–33.

Cacciottolo M, Belcastro V, Laval S, Bushby K, di Bernardo D, Nigro V. Reverse engineering gene network identifies new dysferlin–interacting proteins. Journal of Biological Chemistry 2010;286:5404–13.

Cagliani R, Magri F, Toscano A, Merlini L, Fortunato F, Lamperti C, Rodolico C, Prelle A, Sironi M, Aguennouz M, Ciscato P, Uncini A, Moggio M, Bresolin N, Comi GP. Mutation finding in patients with dysferlin deficiency and role of the dysferlin interacting proteins annexin A1 and A2 in muscular dystrophies. Human Mutation 2005;26:283.

Cai C, Masumiya H, Weisleder N, Matsuda N, Nishi M, Hwang M, Ko JK, Lin P, Thornton A, Zhao X, Pan Z, Komazaki S, Brotto M, Takeshima H, Ma J. MG53 nucleates assembly of cell membrane repair machinery. Nature Cell Biology 2009a;11:56–64.

Cai C, Weisleder N, Ko JK, Komazaki S, Sunada Y, Nishi M, Takeshima H, Ma J. Membrane repair defects in muscular dystrophy are linked to altered interaction between MG53, caveolin-3, and dysferlin. Journal of Biological Chemistry 2009b;284:15894–902.

Campanaro S, Romualdi C, Fanin M, Celegato B, Pacchioni B, Trevisan S, Laveder P, De Pitta C, Pegoraro E, Hayashi YK, Valle G, Angelini C, Lanfranchi G. Gene expression profiling in dysferlinopathies using a dedicated muscle microarray. Human Molecular Genetics 2002;11:3283–98.

Collins JH, Tarcsafalvi A, Ikemoto N. Identification of a region of calsequestrin that binds to the junctional face membrane of sarcoplasmic reticulum. Biochemical and Biophysical Research Communications 1990;167:189–93.

Davis DB, Doherty KR, Delmonte AJ, McNally EM. Calcium-sensitive phospholipid binding properties of normal and mutant ferlin C2 domains. Journal of Biological Chemistry 2002;277:22883–8.

De Luna N, Gallardo E, Illa I. In vivo and in vitro dysferlin expression in human muscle satellite cells. Journal of Neuropathology and Experimental Neurology 2004;63:1104–13.

de Luna N, Gallardo E, Soriano M, Dominguez-Perles R, de la Torre C, Rojas-Garcia R, Garcia-Verdugo JM, Illa I. Absence of dysferlin alters myogenin expression and delays human muscle differentiation in vitro. Journal of Biological Chemistry 2006;281:17092–8.

de Morree A, Hensbergen PJ, van Haagen HH, Dragan I, Deelder AM, t Hoen PA, Frants RR, van der Maarel SM. Proteomic analysis of the dysferlin protein complex unveils its importance for sarcolemmal maintenance and integrity. PLoS ONE 2010;5:e13854.

Demonbreun AR, Fahrenbach JP, Deveaux K, Earley JU, Pytel P, McNally EM. Impaired muscle growth and response to insulin-like growth factor 1 in dysferlin-mediated muscular dystrophy. Human Molecular Genetics 2010;20:779–89.

Di Fulvio S, Azakir BA, Therrien C, Sinnreich M. Dysferlin interacts with histone deacetylase 6 and increases alpha-tubulin acetylation. PLoS ONE 2011;6:e28563.

Dompierre JP, Godin JD, Charrin BC, Cordelieres FP, King SJ, Humbert S, Saudou F. Histone deacetylase 6 inhibition compensates for the transport deficit in Huntington's disease by increasing tubulin acetylation. Journal of Neuroscience 2007;27:3571–83.

Dujardin DL, Barnhart LE, Stehman SA, Gomes ER, Gundersen GG, Vallee RB. A role for cytoplasmic dynein and LIS1 in directed cell movement. Journal of Cell Biology 2003;163:1205–11.

Fliegel L, Ohnishi M, Carpenter MR, Khanna VK, Reithmeier RA, MacLennan DH. Amino acid sequence of rabbit fast-twitch skeletal muscle calsequestrin deduced from cDNA and peptide sequencing. Proceedings of the National Academy of Sciences of the United States of America 1987;84:1167–71.

Förster VT, Mielczarek EV, Greenbaum E, Knox RS. Intermolecular energy migration and fluorescence (Translation of Förster, T., 1948). In: Biological Physics. American Institute of Physics; 1948. p. 183–221.

Glover L, Brown RH Jr. Dysferlin in membrane trafficking and patch repair. Traffic 2007;8:785–94.

Guardia-Laguarta C, Coma M, Pera M, Clarimon J, Sereno L, Agullo JM, Molina-Porcel L, Gallardo E, Deng A, Berezovska O, Hyman BT, Blesa R, Gomez-Isla T, Lleo A. Mild cholesterol depletion reduces amyloid-beta production by impairing APP trafficking to the cell surface. Journal of Neurochemistry 2009;110:220–30.

Haase H, Podzuweit T, Lutsch G, Hohaus A, Kostka S, Lindschau C, Kott M, Kraft R, Morano I. Signaling from beta-adrenoceptor to L-type calcium channel: identification of a novel cardiac protein kinase A target possessing similarities to AHNAK. FASEB Journal 1999;13:2161–72.

Hernandez-Deviez DJ, Howes MT, Laval SH, Bushby K, Hancock JF, Parton RG. Caveolin regulates endocytosis of the muscle repair protein, dysferlin. Journal of Biological Chemistry 2008;283:6476–88.

Hohaus A, Person V, Behlke J, Schaper J, Morano I, Haase H. The carboxyl-terminal region of ahnak provides a link between cardiac L-type Ca^{2+} channels and the actin-based cytoskeleton. FASEB Journal 2002;16:1205–16.

Huang Y, Verheesen P, Roussis A, Frankhuizen W, Ginjaar I, Haldane F, Laval S, Anderson LV, Verrips T, Frants RR, de Haard H, Bushby K, den Dunnen J, van der Maarel SM. Protein studies in dysferlinopathy patients using llama-derived antibody fragments selected by phage display. European Journal of Human Genetics: EJHG 2005;13:721–30.

Huang Y, Laval SH, van Remoortere A, Baudier J, Benaud C, Anderson LV, Straub V, Deelder A, Frants RR, den Dunnen JT, Bushby K, van der Maarel SM. AHNAK, a novel component of the dysferlin protein complex, redistributes to the cytoplasm with dysferlin during skeletal muscle regeneration. FASEB Journal 2007;21:732–42.

Huang Y, de Morree A, van Remoortere A, Bushby K, Frants RR, Dunnen JT, van der Maarel SM. Calpain 3 is a modulator of the dysferlin protein complex in skeletal muscle. Human Molecular Genetics 2008;17:1855–66.

Illa I, Serrano-Munuera C, Gallardo E, Lasa A, Rojas-Garcia R, Palmer J, Gallano P, Baiget M, Matsuda C, Brown RH. Distal anterior compartment myopathy: a dysferlin mutation causing a new muscular dystrophy phenotype. Annals of Neurology 2001;49:130–4.

Illa I, De Luna N, Dominguez-Perles R, Rojas-Garcia R, Paradas C, Palmer J, Marquez C, Gallano P, Gallardo E. Symptomatic dysferlin gene mutation carriers: characterization of two cases. Neurology 2007;68:1284–9.

Klinge L, Harris J, Sewry C, Charlton R, Anderson L, Laval S, Chiu YH, Hornsey M, Straub V, Barresi R, Lochmuller H, Bushby K. Dysferlin associates with the developing T-tubule system in rodent and human skeletal muscle. Muscle and Nerve 2010;41:166–73.

Krahn M, Beroud C, Labelle V, Nguyen K, Bernard R, Bassez G, Figarella-Branger D, Fernandez C, Bouvenot J, Richard I, Ollagnon-Roman E, Bevilacqua JA, Salvo E, Attarian S, Chapon F, Pellissier JF, Pouget J, Hammouda el H, Laforet P, Urtizberea JA, Eymard B, Leturcq F, Levy N. Analysis of the DYSF mutational spectrum in a large cohort of patients. Human Mutation 2009;30:E345–75.

Lennon NJ, Kho A, Bacskai BJ, Perlmutter SL, Hyman BT, Brown RH Jr. Dysferlin interacts with annexins A1 and A2 and mediates sarcolemmal wound-healing. Journal of Biological Chemistry 2003;278:50466–73.

Liu J, Aoki M, Illa I, Wu C, Fardeau M, Angelini C, Serrano C, Urtizberea JA, Hentati F, Hamida MB, Bohlega S, Culper EJ, Amato AA, Bossie K, Oeltjen J, Bejaoui K, McKenna-Yasek D, Hosler BA, Schurr E, Arahata K, de Jong PJ, Brown RH Jr. Dysferlin, a novel skeletal muscle gene, is mutated in Miyoshi myopathy and limb girdle muscular dystrophy. Nature Genetics 1998;20:31–6.

Madaro L, Marrocco V, Fiore P, Aulino P, Smeriglio P, Adamo S, Molinaro M, Bouche M. PKCtheta signaling is required for myoblast fusion by regulating the expression of caveolin-3 and beta1D integrin upstream focal adhesion kinase. Molecular Biology of the Cell 2011;22:1409–19.

Matsuda C, Hayashi YK, Ogawa M, Aoki M, Murayama K, Nishino I, Nonaka I, Arahata K, Brown RH Jr. The sarcolemmal proteins dysferlin and caveolin-3 interact in skeletal muscle. Human Molecular Genetics 2001;10:1761–6.

Matsuda C, Kameyama K, Tagawa K, Ogawa M, Suzuki A, Yamaji S, Okamoto H, Nishino I, Hayashi YK. Dysferlin interacts with affixin (beta-parvin) at the sarcolemma. Journal of Neuropathology and Experimental Neurology 2005;64:334–40.

Minetti C, Sotgia F, Bruno C, Scartezzini P, Broda P, Bado M, Masetti E, Mazzocco M, Egeo A, Donati MA, Volonte D, Galbiati F, Cordone G, Bricarelli FD, Lisanti MP, Zara F. Mutations in the caveolin-3 gene cause autosomal dominant limb-girdle muscular dystrophy. Nature Genetics 1998;18:365–8.

Miyoshi K, Kawai H, Iwasa M, Kusaka K, Nishino H. Autosomal recessive distal muscular dystrophy as a new type of progressive muscular dystrophy. Seventeen cases in eight families including an autopsied case. Brain 1986;109(Pt 1):31–54.

Murphy RM, Larkins NT, Mollica JP, Beard NA, Lamb GD. Calsequestrin content and SERCA determine normal and maximal Ca^{2+} storage levels in sarcoplasmic reticulum of fast- and slow-twitch fibres of rat. Journal of Physiology 2009;587:443–60.

Nguyen K, Bassez G, Krahn M, Bernard R, Laforet P, Labelle V, Urtizberea JA, Figarella-Branger D, Romero N, Attarian S, Leturcq F, Pouget J, Levy N, Eymard B. Phenotypic study in 40 patients with dysferlin gene mutations: high frequency of atypical phenotypes. Archives of Neurology 2007;64:1176–82.

Paradas C, Gonzalez-Quereda L, De Luna N, Gallardo E, Garcia-Consuegra I, Gomez H, Cabello A, Illa I, Gallano P. A new phenotype of dysferlinopathy with congenital onset. Neuromuscular Disorders: NMD 2009;19:21–5.

Paradas C, Llauger J, Diaz-Manera J, Rojas-Garcia R, De Luna N, Iturriaga C, Marquez C, Uson M, Hankiewicz K, Gallardo E, Illa I. Redefining dysferlinopathy phenotypes based on clinical findings and muscle imaging studies. Neurology 2010;75:316–23.

Passos-Bueno MR, Bashir R, Moreira ES, Vainzof M, Marie SK, Vasquez L, Iughetti P, Bakker E, Keers S, Stephenson A, Strachan T, Mahneh I, Weissenbach J, Bushby K, Zatz M. Confirmation of the 2p locus for the mild autosomal recessive limb-girdle muscular dystrophy gene (LGMD2B) in three families allows refinement of the candidate region. Genomics 1995;27:192–5.

Piccolo F, Moore SA, Ford GC, Campbell KP. Intracellular accumulation and reduced sarcolemmal expression of dysferlin in limb – girdle muscular dystrophies. Annals of Neurology 2000;48:902–12.

Roche JA, Ru LW, O'Neill AM, Resneck WG, Lovering RM, Bloch RJ. Unmasking potential intracellular roles for dysferlin through improved immunolabeling methods. Journal of Histochemistry and Cytochemistry 2011;59:964–75.

Royer L, Rios E. Deconstructing calsequestrin. Complex buffering in the calcium store of skeletal muscle. Journal of Physiology 2009;587:3101–11.

Shevchenko A, Tomas H, Havlis J, Olsen JV, Mann M. In-gel digestion for mass spectrometric characterization of proteins and proteomes. Nature Protocols 2006;1:2856–60.

Sun Y, Hays NM, Periasamy A, Davidson MW, Day RN. Monitoring protein interactions in living cells with fluorescence lifetime imaging microscopy. Methods in Enzymology 2011;504:371–91.

Therrien C, Di Fulvio S, Pickles S, Sinnreich M. Characterization of lipid binding specificities of dysferlin C2 domains reveals novel interactions with phosphoinositides. Biochemistry 2009;48:2377–84.

Vale RD. The molecular motor toolbox for intracellular transport. Cell 2003;112:467–80.

Waddell LB, Lemckert FA, Zheng XF, Tran J, Evesson FJ, Hawkes JM, Lek A, Street NE, Lin P, Clarke NF, Landstrom AP, Ackerman MJ, Weisleder N, Ma J, North KN, Cooper ST. Dysferlin, annexin A1, and mitsugumin 53 are upregulated in muscular dystrophy and localize to longitudinal tubules of the T-system with stretch. Journal of Neuropathology and Experimental Neurology 2011;70:302–13.

Zacharias U, Purfurst B, Schowel V, Morano I, Spuler S, Haase H. Ahnak1 abnormally localizes in muscular dystrophies and contributes to muscle vesicle release. Journal of Muscle Research and Cell Motility 2011;32:271–80.

Zhu H, Lin P, De G, Choi KH, Takeshima H, Weisleder N, Ma J. Polymerase transcriptase release factor (PTRF) anchors MG53 protein to cell injury site for initiation of membrane repair. Journal of Biological Chemistry 2011;286:12820–4.